Figure S1.

A

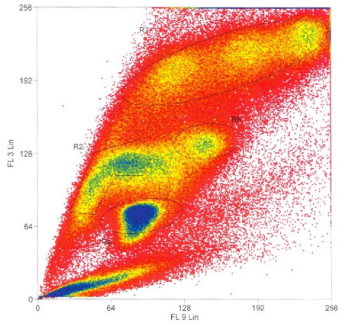

B

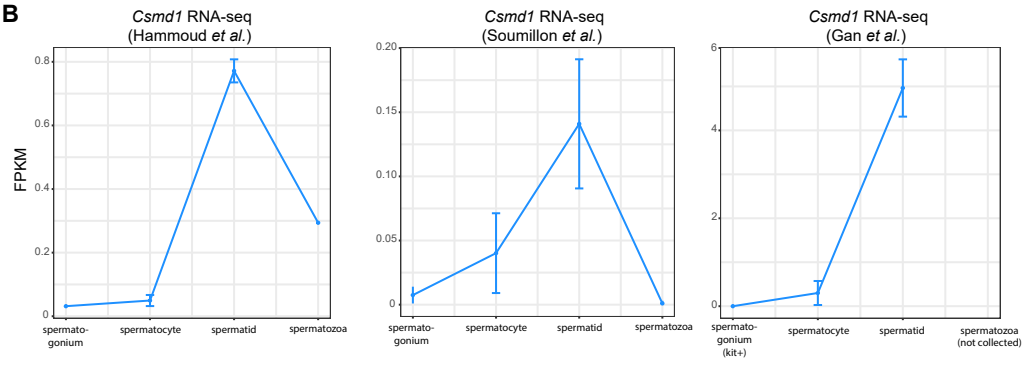

C

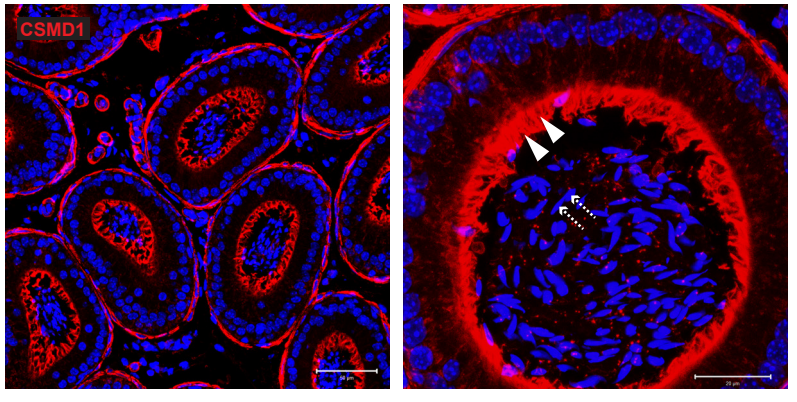

Figure S1. Separating whole tissue into purified germ cell populations and validating *Csmd1* expression patterns, related to Figure 2.

(A) Representative bivariate plot depicting clustering of dissociated germ cells based on intensity of red (x-axis) and blue (y-axis) fluorescence. Due to the size and ploidy changes that accompany normal spermatogenesis, germ cells cluster along the red/blue spectra in a predictable and reproducible manner. Clusters corresponding to spermatogonia, primary spermatocytes, secondary spermatocytes, and spermatids are marked by single, double, triple, and quadruple black arrowheads, respectively. These purified germ cells were collected and sequenced as shown in **Figure 2**.

(B) We validated our RNA-seq data by analyzing RNA expression of *Csmd1* in FPKM of purified spermatogonia, spermatocytes, spermatids, and spermatozoa from previously published resources (Cell Rep. 27:2179-90; Cell Stem Cell. 15:239-53; Mol Cell Proteomics. 12:1144-57). The germ cells from these previous studies were purified using orthogonal technologies to our cytometry-based method shown in (**A**) (i.e., enzymatic dispersion, centrifugal elutriation, and surgical dissection). The increasing pattern of expression in spermatogonia, spermatocyte, and spermatid qualitatively matches the RNA-seq data from our study presented in **Figure 2**.

(C) Immunofluorescence images of wildtype male epididymis containing maturing spermatozoa. CSMD1 protein (red) is highly expressed in the epithelial stereocilia of the epididymis (white arrowheads), but not on the spermatozoa (white dashed arrows), consistent with RNA expression data.

Figure S2.

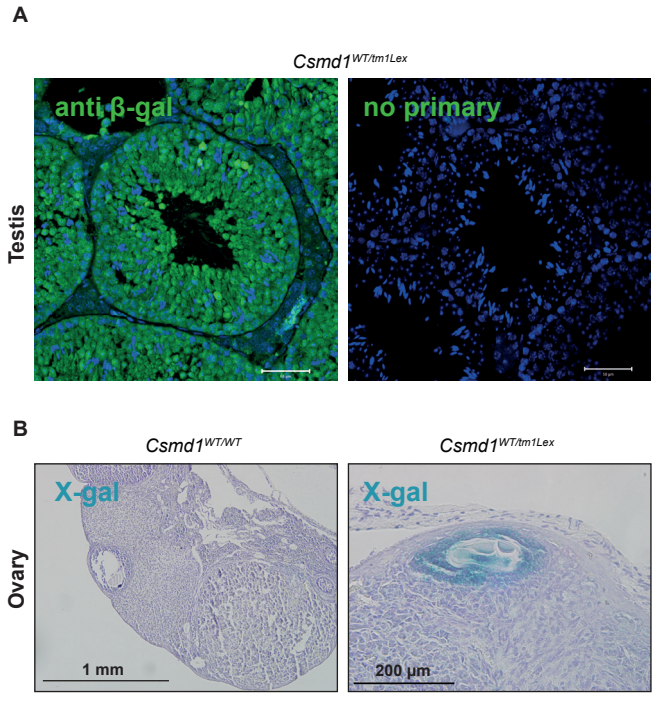
A
Csmd1WT/tm1Lex
anti β-gal
no primary
Testis
B
Csmd1WT/WT
Csmd1WT/tm1Lex
X-gal
X-gal
Ovary
1 mm
200 µm

Figure S2. Independent validation of α-CSMD1 localization, related to Figure 2.

Our *Csmd1* deletion construct incorporates a lacZ reporter cassette. Therefore, we evaluated β-gal expression in (**A**) testis and (**B**) ovary using anti-β-gal antibody and X-gal staining solution, respectively. As expected we do not detect any positive β-gal signal in *Csmd1* wildtype, which does not carry the lacZ cassette. β-gal expression approximates patterns of wildtype α-CSMD1 IF expression shown in **Figure 2**.

Figure S3.

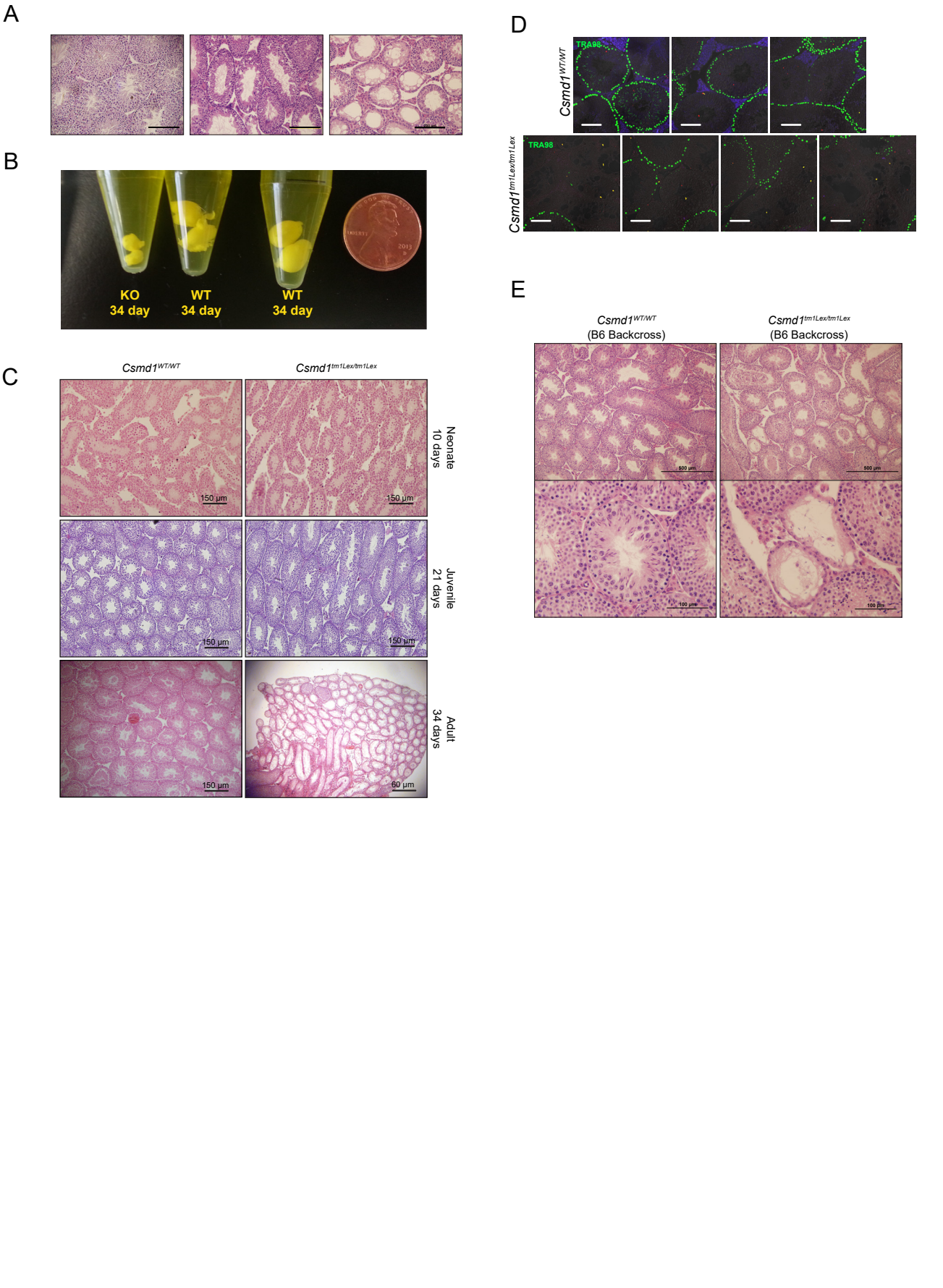
A
B
KO
34 day
WT
34 day
WT
34 day
C
Csmd1WT/WT
Csmd1tm1Lex/tm1Lex
Neonate
10 days
Juvenile
21 days
Adult
34 days
150 µm
60 µm
D
Csmd1WT/WT
Csmd1tm1Lex/tm1Lex
TRA98
E
Csmd1WT/WT
(B6 Backcross)
Csmd1tm1Lex/tm1Lex
(B6 Backcross)
500 µm
100 µm

Figure S3. Detailed pathologic characterization of *Csmd1* knockout testes, related to Figure 3.

(A) *Csmd1* KO testes show heterogeneity in timing, location, and severity of histopathology. Representative examples of tubules scored for quantification in **Figure 3C**. Testes demonstrating no damage ("none") show minimal loss of germ cells and tubules display spatial organization of spermatogenesis. Testes demonstrating "mild" damage display noticeable loss of germ cells, but many tubules maintain some degree of spatial organization. Testes demonstrating "profound" damage have lost many or all germ cells (Sertoli cell-only) and/or display severe loss of spatial organization.

(B) Gross morphology of *Csmd1* wildtype and knockout testes. Left to right: *Csmd1* knockout, wildtype, and wildtype littermates sacrificed at 34 days of age. Corresponding histology for these individuals is presented in **Figure 3A**.

(C) No evidence of testes degeneration prior to sexual maturity. Histological sections of *Csmd1* wildtype (left column) and knockout (right column) during the neonatal (10 days), juvenile (21 days) and adult (34 days) time periods. Neonate and juvenile samples are not yet sexually mature, as they have not completed the first round of spermatogenesis, evidenced by the absence of mature elongated spermatids. *Csmd1* is maximally expressed at the spermatid stage.

(D) Germ-cell marker TRA98 is underexpressed in knockout testes. Immunofluorescence for antibody against TRA98 (green) in *Csmd1* wildtype (upper panels) and knockout (lower panels) littermate testes. The number of TRA98-positive cells ($mean_{wt}$ = 60.3, $mean_{ko}$ = 144), is significantly lower in knockout tubules after normalising for total cell number ($P < 2 \times 10^{-16}$; Poisson regression). All scale bars correspond to 350 μm.

(E) Degeneration is recapitulated in F5 backcrossed knockout testes. We serially backcrossed the *Csmd1*^{tm1Lex} allele onto a homogenous C57BL/6 background for 5 generations and examined histological sections of a set of young (< 2 months) wildtype and knockout littermates. Two out

of two knockout samples showed evidence of moderate to severe degeneration in a subset of the tubules.

Figure S4.

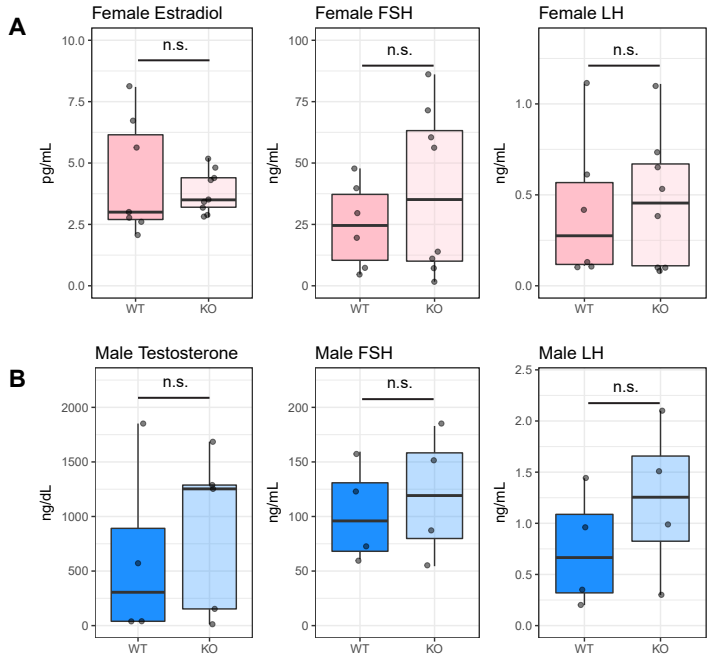
A
Female Estradiol
n.s.
pg/mL
10.0
7.5
5.0
2.5
0.0
WT
KO
Female FSH
n.s.
ng/mL
100
75
50
25
0
WT
KO
Female LH
n.s.
ng/mL
1.0
0.5
0.0
WT
KO
B
Male Testosterone
n.s.
ng/dL
2000
1500
1000
500
0
WT
KO
Male FSH
n.s.
ng/mL
200
150
100
50
0
WT
KO
Male LH
n.s.
ng/mL
2.5
2.0
1.5
1.0
0.5
0.0
WT
KO

Figure S4. Male and female sex hormone measurements, related to Figure 4.

Boxplots depicting sex hormone measurements along the pituitary-gonadal axis in **(A)** females (estradiol, FSH, and LH) and **(B)** males (testosterone, FSH, and LH). No significant differences in hormone levels were detected between wildtypes and knockouts (Student's *t*-test).

Figure S5.

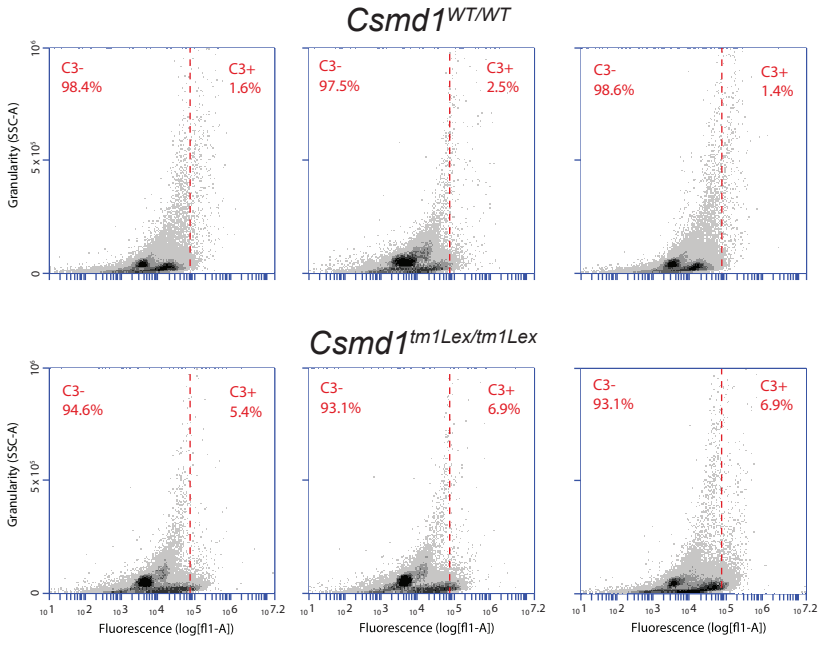
Csmd1WT/WT
C3-
98.4%
C3+
1.6%
C3-
97.5%
C3+
2.5%
C3-
98.6%
C3+
1.4%
Granularity (SSC-A)
Csmd1tm1Lex/tm1Lex
C3-
94.6%
C3+
5.4%
C3-
93.1%
C3+
6.9%
C3-
93.1%
C3+
6.9%
Fluorescence (log[fl1-A])

Figure S5. C3 deposition in *Csmd1* wildtype versus knockout testes, related to Figure 6.

FACS output depicting total C3 deposition on *Csmd1* wildtype and knockout testes collected with identical gating parameters.

Figure S6.

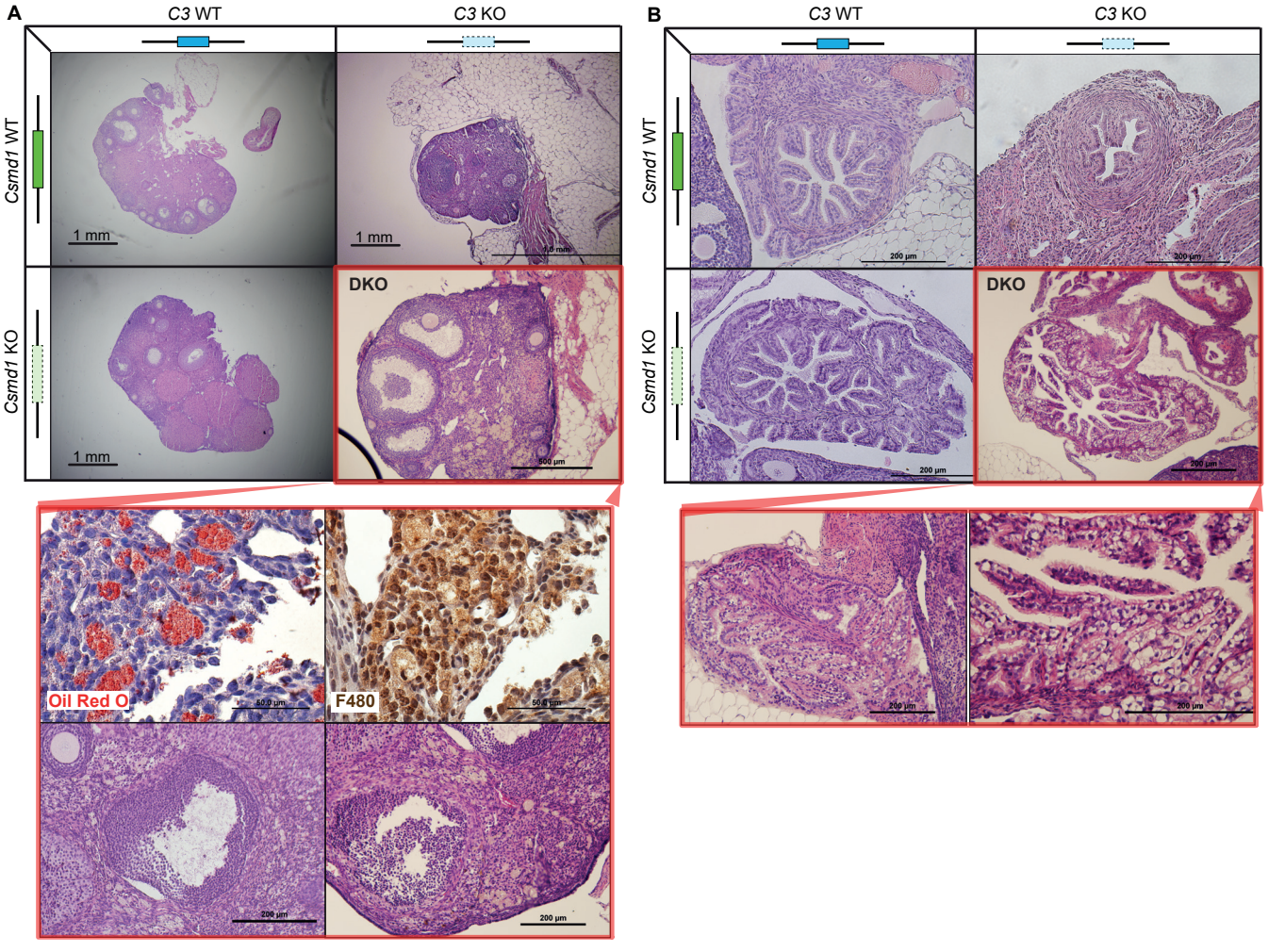
A
C3 WT
C3 KO
Csmd1 WT
Csmd1 KO
1 mm
1 mm
1 mm
DKO
500 µm
Oil Red O
50.0 µm
F480
50.0 µm
200 µm
200 µm
B
C3 WT
C3 KO
Csmd1 WT
Csmd1 KO
200 µm
200 µm
200 µm
DKO
200 µm
200 µm
200 µm

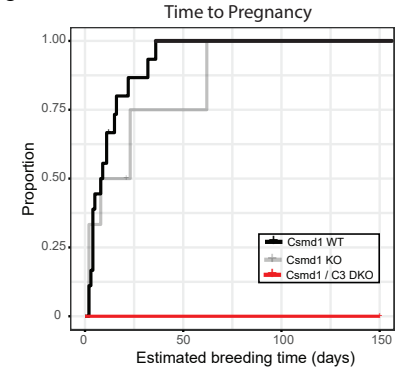
C
Time to Pregnancy
Proportion
1.00
0.75
0.50
0.25
0
0
50
100
150
Estimated breeding time (days)
Csmd1 WT
Csmd1 KO
Csmd1 / C3 DKO

Figure S6. Complement deficiency unmasks severe morphological derangement in *Csmd1* knockout ovaries, related to Figure 6.

(A) Example H&E ovarian histology of *C3* and *Csmd1* wildtype/knockout combinations. Closer inspection of *C3/Csmd1* double knockout ovaries shows profound inflammatory changes of the germ cells and surrounding stroma with associated foam cell macrophages which stain positively for Oil Red O and F4/80. Follicle shape is grossly deformed.

(B) H&E histology of *C3/Csmd1* double knockout oviducts showing severe derangement of the epithelial mucosa.

(C) Timed breeding compares mating success among *Csmd1* wildtype (black), *Csmd1* knockout (grey), and *C3*/*Csmd1* double knockout (red) females. *C3*/*Csmd1* double knockout females produced zero offspring after > 5 months of breeding. A subset of *Csmd1* WT and KO breeding data are replotted from Figure 4 for ease of comparison.